Anal. Chem. **2010,** *82,* 3146–3154

The Effect of AC Frequency on the Electrowetting Behavior of Ionic Liquids

Yasith S. Nanayakkara,[†] Sirantha Perera,[†] Shreyas Bindiganavale,[‡] Eranda Wanigasekara,[†] Hyejin Moon,*[,‡] and Daniel W. Armstrong*[,†]

Department of Chemistry and Biochemistry, and Department of Mechanical and Aerospace Engineering, The University of Texas at Arlington, Arlington, Texas 76019

This paper presents a study of electrowetting of ionic liquids (ILs) under AC voltages, where nine different ILs (including mono-, di-, and tricationic varieties) with three different AC frequencies (60 Hz, 1 kHz, 10 kHz) were experimentally investigated. The main foci of this study are (i) an investigation of AC frequency dependence on the electrowetting of ILs; (ii) obtaining theoretical relationships between the relevant factors that explain the experimentally achieved frequency dependence; and (iii) a systematic comparison of electrowetting of ILs using AC vs DC voltage fields. The frequency of the AC voltage was found to be directly related to the apparent contact angle change ($\Delta\theta$) of the ILs. This relationship was further analyzed and explained theoretically. The electrowetting properties of ILs under AC voltages were compared to that under DC voltages. All tested ILs showed greater apparent contact angle changes with AC voltage conditions than with DC voltage conditions. The effect of structure and charge density also was examined. Electrowetting reversibility under AC voltage conditions was studied for few ILs. Finally, the physical properties and AC electrowetting properties of ILs were measured and tabulated.

Electrowetting is a well-known phenomenon in which a liquid drop spreads on a solid surface upon application of an electric field across the liquid/solid interface. The spreading of a liquid drop by an electric field is often observed on dielectric coated surfaces as well as conductive solid surfaces. In either case, one of the conventional methods to measure the extent of electrowetting is measuring the change in apparent (macroscopic) contact angle.[1] When a liquid drop on a solid surface spreads due to electric field, its apparent contact angle decreases. Since our measurements are apparent contact angles (not intrinsic contact angles), herein we will use "contact angle" to refer the "apparent contact angle." If electrowetting is performed on a smooth dielectric solid (e.g., Teflon), when the voltage is removed from the system, the contact angle will tend to approach its original value.[2,3] Electrowetting on dielectric (EWOD) is popular because of its usefulness in droplet based microfluidic devices or digital microfluidics.[4,5] Drop actuation using EWOD in laboratory-on-a-chip platforms is relatively trouble-free and inexpensive compared to traditional pump and microchannel based laboratory-on-a-chip platforms. Indeed they have been used successfully in the preparation of biological samples as well as for some analytical processes.[6−11] Other than microfluidics, electrowetting is used in fluid focal lenses,[12] electrowetting displays,[13] programmable optical filters,[14] paint drying,[14] micromotors,[15] electronic microreactors,[16] and to control fluids in multichannel structures.[17]

There are some significant advantages of ILs as compared to water and other aqueous electrolytes. ILs have greater stability at elevated temperatures, are liquid over a much wider temperature range, have negligible evaporation, have tunable physical properties and have selective solubility and selective extractability for various organic compounds, metal ions and biological molecules.[2,18] Also corrosion inhibition is achievable for some ILs (however diluted/hygroscopic ILs can facilitate corrosion).[19] In recent studies the electrowetting behavior of ILs was evaluated

* To whom correspondence should be addressed. Phone: (817) 272-0632. Fax: (817) 272-0619. E-mail: hyejin.moon@uta.edu (H.M.); sec4dwa@uta.edu (D.W.A.).
[†] Department of Chemistry and Biochemistry.
[‡] Department of Mechanical and Aerospace Engineering.

(1) Mugele, F.; Buehrle, J. *J. Phys.: Condens.Matter* **2007**, *19*, 375112/1–375112/20.
(2) Nanayakkara, Y. S.; Moon, H.; Payagala, T.; Wijeratne, A. B.; Crank, J. A.; Sharma, P. S.; Armstrong, D. W. *Anal. Chem.* **2008**, *80*, 7690–7698.
(3) Millefiorini, S.; Tkaczyk, A. H.; Sedev, R.; Efthimiadis, J.; Ralston, J. *J. Am. Chem. Soc.* **2006**, *128*, 3098–3101.
(4) Pollack, M. G.; Fair, R. B.; Shenderov, A. D. *Appl. Phys. Lett.* **2000**, *77*.
(5) Cho, S. K. *J. Microelectromech. Syst.* **2003**, *12*, 70–80.
(6) Srinivasan, V.; Pamula, V. K.; Fair, R. B. *Lab Chip* **2004**, *4*, 310–315.
(7) (a) Srinivasan, V.; Pamula, V. K.; Fair, R. B. *Anal. Chim. Acta* **2004**, *507*, 145–150. (b) Srinivasan, V.; Pamula, V.; Pollack, M.; Fair, R. *Proceedings of 16th Annual IEEE International Conference on MEMS*, Kyoto, Japan, January 19−23, 2003; pp 327−330.
(8) Wheeler, A. R.; Moon, H.; Kim, C.-J.; Loo, J. A.; Garrell, R. L. *Anal. Chem.* **2004**, *76*, 4833–4838.
(9) Yoon, J.-Y.; Garrell, R. L. *Anal. Chem.* **2003**, *75*, 5097–5102.
(10) Wheeler, A. R.; Moon, H.; Bird, C. A.; Ogorzalek Loo, R. R.; Kim, C.-J.; Loo, J. A.; Garrell, R. L. *Anal. Chem.* **2005**, *77*, 534–540.
(11) Moon, H.; Wheeler, A. R.; Garrell, R. L.; Loo, J. A.; Kim, C. *Lab Chip* **2006**, *6*, 1213–1219.
(12) Berge, B.; Peseux, J. *Eur. Phys. J. E* **2000**, *3*, 159–163.
(13) Hayes, R. A.; Feenstra, B. J. *Nature* **2003**, *425*, 383–385.
(14) Welters, W. J. J.; Fokkink, L. G. J. *Langmuir* **1998**, *14*, 1535–1538.
(15) Lee, Junghoon *MEMS 98. Proceedings. The Eleventh Annual International Workshop on*; Micro Electro Mechanical Systems: Heidelberg, January 25−29, 1998; pp 538−543.
(16) Dubois, P.; Marchand, G.; Fouillet, Y.; Berthier, J.; Douki, T.; Hassine, F.; Gmouh, S.; Vaultier, M. *Anal. Chem.* **2006**, *78*, 4909–4917.
(17) Huh, D.; Tkaczyk, A. H.; Bahng, J. H.; Chang, Y.; Wei, H.-H.; Grotberg, J. B.; Kim, C.-J.; Kurabayashi, K.; Takayama, S. *J. Am. Chem. Soc.* **2003**, *125*, 14678–14679.
(18) Soukup-Hein, R. J.; Warnke, M. M.; Armstrong, D. W. *Annu. Rev. Anal. Chem.* **2009**, *2*, 145–168.
(19) Uerdingen, M.; Treber, C.; Balser, M.; Schmitt, G.; Werner, C. *Green Chem.* **2005**, *7*, 321–325.

10.1021/ac9021852
Published on Web 03/29/2010

under DC conditions.[2,3,20−22] In addition ILs have been used under AC conditions for some EWOD based applications, such as on digital microfluidic devices,[23] electronic microreactors,[16] micro heat transfer devices,[24] and liquid−liquid extraction devices.[25] In our previous work the effects of IL structure on their electrowetting behavior were studied systematically under DC conditions.[2] In this work we focus on the electrowetting of ILs under AC voltage at three different frequencies. Nine different ILs, including mono, di, and tricationic ILs were tested. Among them two are phosphonium based ILs, one is a pyrrolidinium based IL and the others are imidazolium based ILs. Previous studies have shown that electrowetting of water and simple electrolytes under AC voltage can have very different behaviors than with DC voltages.[26−31] However electrowetting behaviors of ILs under AC voltage conditions have not yet been studied to our knowledge. This study provides substantial information for designing and optimizing the properties of ionic liquids for electrowetting purposes. This opens up more potential applications of electrowetting based microfluidic devices which is currently limited in aqueous based solution operations.

Theoretical Background. Contact angle change by electrowetting can be described by a combination of Young's equation and Lippmann's equation (eq 1).[2]

$$\cos\theta = \cos\theta_0 + \frac{c}{2\gamma}V_D^2 = \cos\theta_0 + \frac{\varepsilon\varepsilon_0}{2\gamma t}V_D^2 \qquad (1)$$

Here, V_D is the voltage across the dielectric layer, c is the specific capacitance (capacitance per unit area), ϵ is the relative permittivity of the dielectric layer (dielectric constant), ϵ_0 is the permittivity of free space, γ is the surface tension of the liquid, t is the thickness of the dielectric layer, θ is the contact angle at a designated voltage and/or frequency and θ_0 is the contact angle at zero external voltage. According to eq 1 an increase of voltage should decrease the contact angle value. However upon increasing the voltage at some point (voltage) the contact angle stops changing (Figure 1a). That point is referred to as "saturation point", and accordingly the saturation voltage and saturation angle are the corresponding voltage and corresponding contact angle values respectively. It has been reported

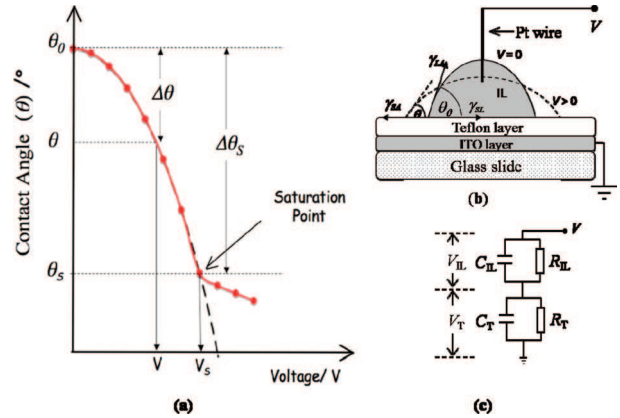

Figure 1. (a) An idealized electrowetting curve obtained by plotting the contact angle of a liquid drop on a dielectric surface versus voltage. θ_0 is the initial contact angle at zero external voltage. θ_S and V_S are saturation contact angle and saturation voltage respectively. $\Delta\theta$ is the apparent contact angle change at any given voltage. $\Delta\theta_S$ is the maximum apparent contact angle change. (b) Experiment setup for electrowetting measurements. Solid line represents the drop shape at zero external voltage. Dashed line represents the drop shape at a given external voltage. γ_{SA}, γ_{LA}, and γ_{SL} are solid-air, liquid−air and solid-air interfacial tensions respectively. (c) Equivalent circuit model for the electrowetting experiment. R is the resistance and C is the capacitance. The subscripts "IL" and "T" indicate IL and Teflon layer, respectively.

that eq 1 predicts the contact angle change due to an electric field relatively well until the saturation point.[2,3]

Five quantities can be identified from contact angle vs voltage plots and used to characterize eletrowetting solvents (Figure 1a). They are as follows: θ_o is the contact angle at zero voltage, θ_s and V_S are the saturation contact angle and saturation voltage, respectively. $\Delta\theta$ is the apparent contact angle change ($\Delta\theta = \theta_o - \theta$) at any voltage and/or frequency. Finally, $\Delta\theta_S$ is the maximum apparent contact angle change ($\Delta\theta_S = \theta_o - \theta_S$).

EXPERIMENTAL SECTION

The acronyms, chemical names, and structures of the ionic liquids used in this work are shown in Figure 2 and some of their relevant physical properties are listed in Table 1. All of the tested ILs were synthesized in our laboratory as reported previously[22,32,33] except for [bmpy][NTf_2], [$3C_6C_{14}P$][DCA], and [$3C_6C_{14}P$][NTf_2]. [Bmpy][NTf_2] was purchased from Sigma-Aldrich (St. Louis, MO). [$3C_6C_{14}P$][DCA] and [$3C_6C_{14}P$][NTf_2] were provided by CYTEC (www.cytec.com, West Paterson, NJ). Both [$3C_6C_{14}P$][DCA] and [$3C_6C_{14}P$][NTf_2] are phosphonium based ILs, [bmpy][NTf_2] is a pyrrolidinium based IL, and the rest are imidazolium based ILs. [$(Bim)_2C_{10}$][NTf_2] is a dicationic ionic liquid, [$(beim)_3a$][NTf_2] is a tricationic ionic liquid with a rigid core, while [$(bimC_{10})_2im$][NTf_2] is a flexible, linear tricationic ionic liquid and the rest of ILs are monocationic ionic liquids. Before the experiments each tested IL was kept in a vacuum oven 12−18 h with phosphorus pentoxide (P_2O_5) at room temperature to minimize the water content. The final

(20) Halka, V.; Freyland, W. *Z. Phys. Chem.* **2008**, *222* (1), 117–127.
(21) Restolho, J.; Mata, J. L.; Saramago, B. *J. Phys. Chem. C* **2009**, *113*, 9321–9327.
(22) Wanigasekara, E.; Zhang, X.; Nanayakkara, Y. S.; Moon, H.; Armstrong, D. W. *Appl. Mater. Interfaces* **2009**, *1* (10), 2126–2133.
(23) Chatterjee, D.; Hetayothin, B.; Wheeler, A. R.; King, D. J.; Garrell, R. L. *Lab Chip* **2006**, *6*, 199–206.
(24) Moon, H.; Bindiganavale, S.; Nanayakkara Y. S.; Armstrong D. W. *Proceedings of the Seventh International ASME Conference on Nanochannels, Microchannels and Minichannels ICNMM2009*; Pohang: South Korea, June 22−24, 2009.
(25) Kunchala, P.; Moon, H.; Nanayakkara Y. S.; Armstrong D. W. *Proceedings of the ASME 2009 Summer Bioengineering Conference (SBC2009)*; Lake Tahoe, CA, June 17−21, 2009.
(26) Quilliet, C.; Berge, B. *Curr. Opin. Colloid Interface Sci.* **2001**, *6*, 34–39.
(27) Blake, T. D.; Clarke, A.; Stattersfield, E. H. *Langmuir* **2000**, *16*, 2928–2935.
(28) Ko, S. H.; Lee, H.; Kang, K. H. *Langmuir* **2008**, *24*, 1094–1101.
(29) Kumar A.; Pluntke M.; Cross B.; Baret J. C.; Mugele F. *Proceedings of the Materials Research Society Fall Meeting*, Boston, November, 2005; E-N06-01.1.
(30) Mugele, F.; Baret, J. *J. Phys.: Condens. Matter* **2005**, *17*, R705–R774.
(31) Hong, J.; Ko, S.; Kang, K.; Kang, I. *Microfluid. Nanofluid.* **2008**, *5*, 263–271.
(32) Anderson, J. L.; Ding, R.; Ellern, A.; Armstrong, D. W. *J. Am. Chem. Soc.* **2005**, *127*, 593–604.
(33) (a) Sharma, P. S.; Payagala, T.; Wanigasekara, E.; Wijeratne, A. B.; Huang, J.; Armstrong, D. W. *Chem. Mater.* **2008**, *20*, 4182–4184. (b) Carda-Broch, S.; Berthod, A.; Armstrong, D. W. *Anal. Bioanal. Chem.* **2003**, *375*, 191–199.

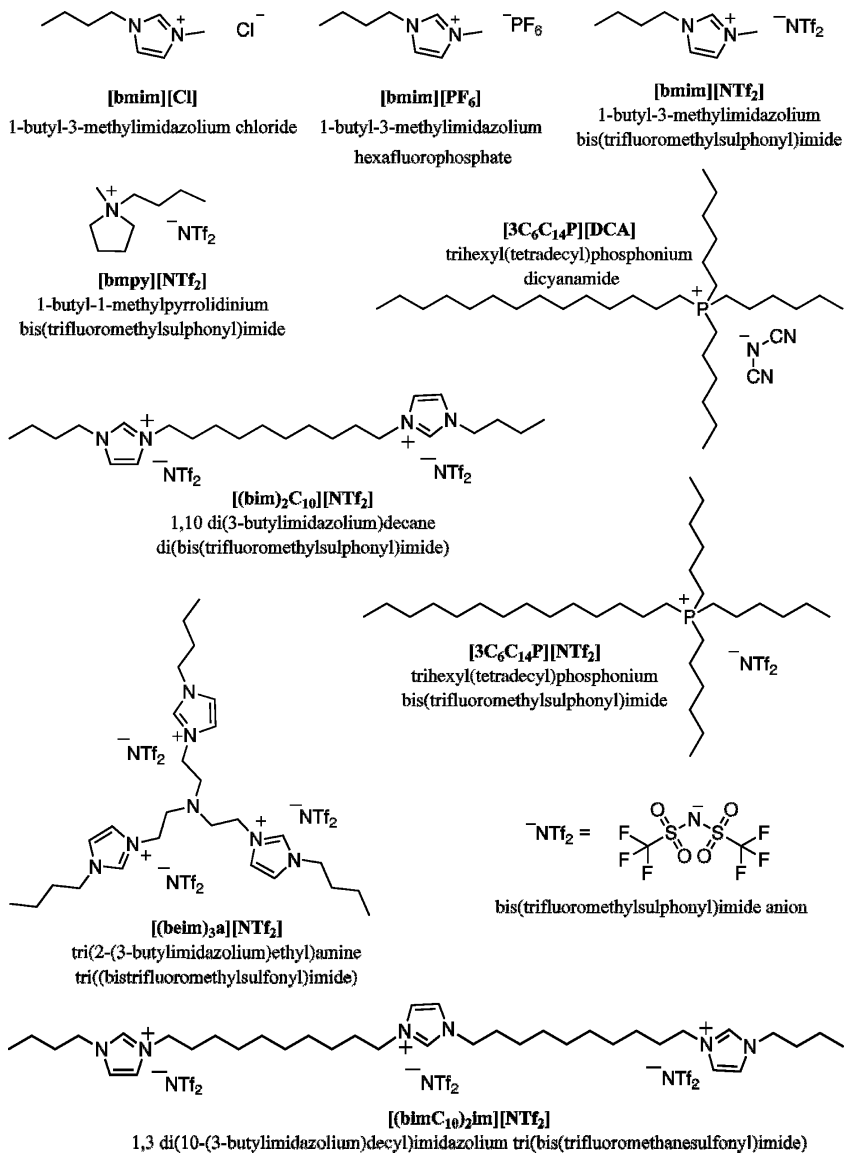

Figure 2. Structures, acronyms, and chemical names of the investigated ionic liquids.

Table 1. Physical Properties of the Studied Ionic Liquids

	ionic liquid[a]								
	[bmim][Cl]	[bmim][PF_6]	[bmim][NTf_2]	[bmpy][NTf_2]	[$3C_6C_{14}P$][NTf_2]	[$3C_6C_{14}P$][DCA]	[$(bim)_2C_{10}$][NTf_2]	[$(beim)_3a$][NTf_2][b]	[$(bimC_{10})_2im$][NTf_2]
MW (g/mol)	174.7	284.2	419.4	422.4	764.0	493.8	884	1311.2	1435.3
melting point (°C)	65[b,c]	−8[b]	−4[b]		>−76<−22[d]	>−76<−22[d]		−47.5	−53.17[e]
[f]density, d (g/cm3)	1.10[b]	1.36[b]	1.43[b]	1.40	1.06[d]	0.90[d]	1.401	1.41	1.54[e]
refractive index	1.523[b]	1.411[b]	1.427[b]		1.451[d]	1.484[d]	1.483	1.451	1.44[e]
[g]viscosity (cSt) 30 °C	1701[b]	170[b]	36[b]		219[d]	269[d]	146	1580	2400[e]
conductivity (x 10^{-4} S/cm) at 25 °C	0.3[h]	14.6[i]	40.6[i]	22[j]	2.1[k]	0.9[k]			
[m]approximate thermal stability	145[b]		185[b]		380[d]	360[d]		308	350[e]
surface tension (dyn/cm)	60.7[b]	44.8[b]	32.8[b]	35.2[n]	31.7[n]	40.8[b]	37.5[p]	43.2	40.4[p]
miscibility with water	M	I	I	I	I	I	I	I	I

[a] Structures and names of ILs are shown in Figure 2. [b] Ref 2. [d] Ref 42. [e] Ref 22. [n] Ref 43. [j] Ref 44. [i] Ref 45. [h] Ref 46. [c] Measured at a supercooled state. [f] Measured using a pycnometer. [g] Measured using a capillary viscometer. [k] Measured using a conductivity meter. [m] Thermogravimetric analysis (TGA), temperature at 1% mass decrease of sample. [p] Measured using a Fisher surface tensiometer (model 20), *I* = immiscible, *M* = miscible.

water content of each IL as measured by Karl Fischer titration is, 1.56% for [bmim][Cl], 990 ppm for [bmim][PF_6], 470 ppm for [bmim][NTf_2], 320 ppm for [bmpy][NTf_2], 0.29% for [$3C_6C_{14}P$][DCA], 420 ppm for [$3C_6C_{14}P$][NTf_2], 480 ppm for [$(bim)_2C_{10}$][NTf_2], 980 ppm for [$(bimC_{10})_2im$][NTf_2], and 810 ppm for [$(beim)_3a$][NTf_2].

The substrate preparation and electrowetting experiments were performed in a similar manner to that reported elsewhere.[2] First,

Table 2. Electrowetting Properties of Studied Ionic Liquids[a]

	[bmim][Cl]	[bmim][PF_6]	[bmim][NTf_2]	[bmpy][NTf_2]	[$3C_6C_{14}P$][DCA]	[$3C_6C_{14}P$][NTf_2]	[$(bim)_2C_{10}$][NTf_2]	[$(beim)_3a$][NTf_2]	[$(bimC_{10})_2im$][NTf_2]
θ_0	98 ± 1	90 ± 1	75 ± 1	79 ± 1	77 ± 1	72	79 ± 1	78 ± 1	80
	θ_S	θ_S	θ_S	θ_S	θ_S	θ_S	θ_S	θ_S	θ_S
DC + ve	[b]80	[b]78	[b]68	71	[b]62	55	64	[b]57	[c]66
DC - ve	[b]84	[b]73	[b]65	66	[b]68	58	60	[b]52	[c]65
60 Hz	77	73	56	58	31	38	32	31	39
1 kHz	58	46	37	42	21	22	30	29	30
10 kHz	53	35	26	40	11	10	39	26	41;29

[a] Extended version of this Table with V_S values, is included in the Supporting Information section. [b] Ref 2. [c] Ref 22.

30 nm thick Indium−tin-oxide (ITO) precoated unpolished float glass slides were used as purchased (www.delta-technologies.com, Stillwater, MN). They were dip coated with an amorphous fluoropolymer layer (Teflon). The Teflon solution was prepared by dissolving 4% (w/v) of Teflon AF1600 (www2.dupont.com, Wilmington, DE) in Fluoroinert FC75 solvent (www.fishersci.com Barrington, IL). The approximate dipping speed of the custom-made dipcoater was 0.78 ± 0.03 mm/s. Dipping was stopped for 5 s, once $^3/_4$ of the slide was dipped in the solution, and then the slide was raised at the same speed. The coated slides were then heat treated serially for 6 min at 112 °C, 5 min at 165 °C and 15 min at 328 °C in an oven. Teflon coated glass slides were then allowed to reach room temperature, washed thoroughly with acetone and deionized water and air-dried. Then the electrowetting experiment was conducted using a contact angle goniometer (CAM 101, www.ksvltd.com, Monroe, CT).

A capillary tube was used to place a drop of ionic liquid (~5 μL) on top of the Teflon layer (Figure 1b). Since ILs are viscous, a micro pipet cannot be used to place/measure the ionic liquid drop. For a specific IL volume variation is approximately ±1 μL. The variation in volumes between different ILs was ±2 μL. However this variation affects neither the contact angle of the drop nor the apparent contact angle change by electrowetting. (See Supporting Information (SI) Figure S3). The volume and the contact angle of the drop were calculated using CAM 200 software (www.ksvltd.com, Monroe, CT). The AC voltage was applied in 5 V increments starting from 0 V, using a waveform generator (Agilent model 33220A) connected to a voltage amplifier (Trek model PZD 350). One electrode was attached to a Pt wire (36 gauge), which was inserted to the drop while the ground electrode was attached to the ITO layer. The voltage was increased in 5 V increments until the IL drop burned, decomposed or oscillated. For each voltage value, the contact angle was measured. This procedure was repeated for each IL at three different frequencies, 60 Hz, 1 and 10 kHz. DC electrowetting experiments were conducted as reported in our previous work on the DC electrowetting of ILs (from 0 to ± 70 V).[2]

The volume and the contact angle of the drop were measured for water, a water miscible IL ([bmim][Cl]), and a water immiscible IL ([bmim][NTf_2]) with time. First a drop of liquid (~5 μL) was placed on the Teflon layer. Then pictures were taken at 5 min interval for 45 min, without applying any external voltage. Subsequently, the volume and contact angle of the drop were calculated and the volume versus time curves and contact angle versus time curves were plotted. The impact of water on the AC electrowetting of ILs was evaluated using both a water-miscible IL (i.e., [bmim][Cl]) and a water-immiscible IL (i.e., [bmim][NTf_2]). 16, 48, and 80% water containing, [bmim][Cl] + water, (w/w) solutions were prepared. Then electrowetting experiments were conducted at 1 kHz for the water containing solutions as well as for the pure DI water. For the water immiscible IL, 0.5 mL of [bmim][NTf_2] was added to 5 mL of water, shaken for 2 min and then allowed to settle for one hour. The water layer was then decanted from the clearly observed two layers. The electrowetting experiments were conducted on the remaining [bmim][NTf_2] layer at all three frequencies (i.e., 60 Hz, 1 kHz, and 10 kHz).

All the experiments were conducted in ambient conditions 23 ± 1 °C and all the AC voltages are reported in V_{rms} values, unless otherwise noted. In regard to their safety, all of the tested ILs are nonflammable.

RESULTS AND DISCUSSION

Initial Contact Angle (θ_0). The θ_0 is the contact angle at zero external voltage therefore, it refers both apparent and intrinsic contact angle if the solid surface is ideally smooth. On such ideal surfaces, θ_0 can be described using the Young equation, where $\theta_0 = \cos^{-1}[(\gamma_{SA} - \gamma_{LS})/\gamma_{LA}]$, where γ_{SA}, γ_{LS}, and γ_{LA} are solid/air, liquid/solid, and liquid/air interfacial tensions, respectively (Figure 1b).[2,34] It has been reported that, for a series of liquids, only the surface tension of the liquid can affect its θ_0 value in identical experimental conditions.[2] Table 2 lists the θ_0 values for all ILs. It is observed that different ILs have different θ_0 values. ILs in this study can be broadly categorized in to three different groups by means of their surface tension values. The surface tensions of [bmim][Cl] and [bmim][PF_6] are higher than 44 dyn/cm (See Table 1), while [bmim][NTf_2] and [$3C_6C_{14}P$][NTf_2] have surface tension values lower than 34 dyn/cm. The surface tensions of the other five ILs lie between 34 dyn/cm and 44 dyn/cm. It was observed that, [bmim][Cl] and [bmim][PF_6] have higher θ_0 values (98° and 90° respectively) than all other ILs (see Table 2). Similarly, [bmim][NTf_2] and [$3C_6C_{14}P$][NTf_2] have lower θ_0 values (75° and 72° respectively) than the other ILs, while other five ILs have intermediate θ_0 values (between 77° and 80°). Therefore it can be concluded that the θ_0 value correlates directly with the surface tension of the IL, i.e., the higher the surface tension of the IL, the higher the θ_0 value obtained.

θ, $\Delta\theta$, V_S, θ_S, and $\Delta\theta_S$ Values. Figure 3 shows the electrowetting curves of [$3C_6C_{14}P$][DCA] at different voltage and frequency conditions. It was observed that, at a given voltage the $\Delta\theta$ values of [$3C_6C_{14}P$][DCA] with AC voltage were always

(34) Wang, W.; Murray, R. W. *Anal. Chem.* **2007**, *79*, 1213–1220.

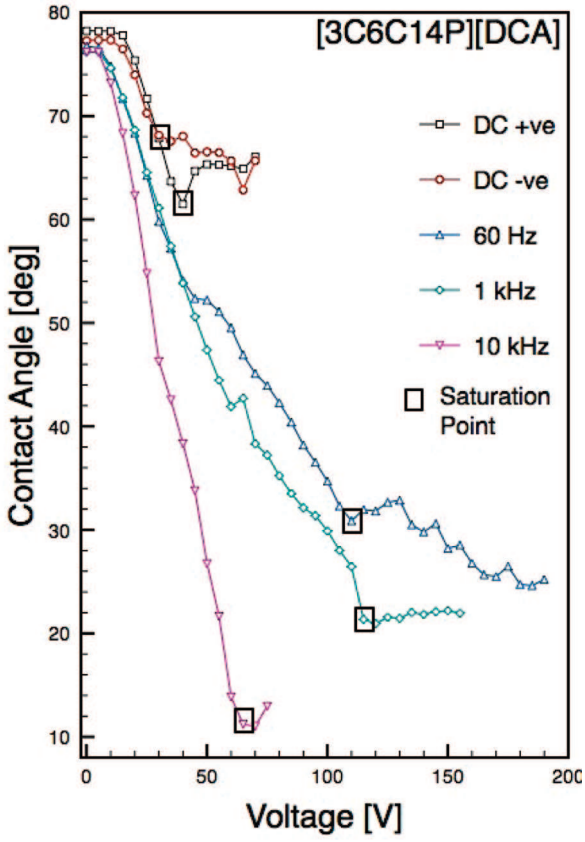

Figure 3. Electrowetting curves of $[3C_6C_{14}P][DCA]$ with DC and AC voltage conditions.

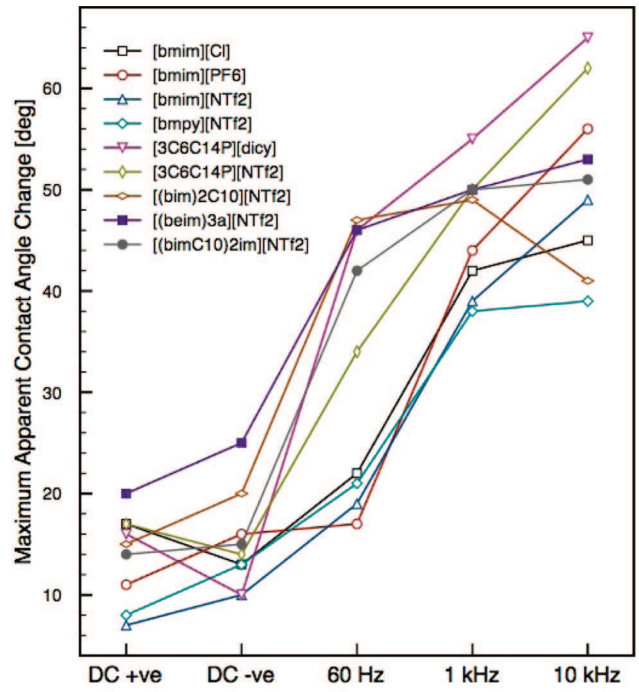

Figure 4. Maximum apparent contact angle change, $\Delta\theta_S$, of ILs at ± DC voltages and three different frequencies of AC voltage.

substantially larger than those with DC voltage (at 60 V_{AC} and 10 kHz, $\Delta\theta$ is more than 5 times larger than the $\Delta\theta$ with +60 V_{DC}). In other words, lower contact angles (θ) can be obtained when using AC voltages as compared to those obtained for DC voltages. Furthermore, it appears that an increase in the AC frequency leads to a further increase in the $\Delta\theta$ value, that is, at higher frequencies, lower θ values are obtained. The behavior is apparent for $[3C_6C_{14}P][DCA]$ at 60 V. It has five different contact angle values; 14°, 42°, 50°, 65°, and 66° at 10 kHz AC, 1 kHz AC, 60 Hz AC, and (+) or (−) DC voltages, respectively. Similar behavior was observed for the all tested ILs. (SI) Figures S4−S11].

Figure 4 shows the $\Delta\theta_S$ of all ILs under both AC and DC voltage conditions and Table 2 lists the corresponding θ_S. It appears that in general $\Delta\theta_S$ increases (i.e., θ_S decreases) with increasing frequency. Also, it is observed that, θ_S in AC conditions is always smaller than that of DC conditions. Finally it was observed that the V_S under DC voltage conditions is generally lower than it is with AC conditions. (See SI Table S1).

Our observations (vidae supra) can be explained using a model similar to that reported by Chatterjee et al.[35] First, the voltage across the dielectric (Teflon) layer, V_D, was determined using the model. (Figure 1c shows the equivalent circuit model for the sessile drop electrowetting experiment). Then, it was combined with the Young-Lippmann equation (eq 1) to establish the relationship with contact angle (θ), in a way similar to that described by Kumar et al.[29] The final derived relationship is

$$\theta = F(V, f, \gamma, \sigma, \varepsilon_{IL}, d) \quad (2)$$

(see SI for the step by step derivation of this expression).

It shows that the contact angle (θ) is a function of externally controlled factors (i.e., applied external voltage (V) and frequency (f)) as well as some physical properties of the IL itself (i.e., surface tension (γ), conductivity (σ), dielectric constant (ε_{IL}), and double layer thickness (d)).

For a given IL, ε_{IL}, σ, γ, and d are constants. During the entire experiment the distance between the Pt tip and the Teflon surface remains constant. Therefore according to eq 2 for a given IL, θ depends only on f and V. This phenomenon can be easily visualized by the electrowetting curves of $[3C_6C_{14}P][DCA]$ in Figure 3. Applying +60 V DC voltage, θ changes from 77° to 65°, which is due to the basic electrowetting effect described by Young and Lippmann's equation (eq 1). While keeping the voltage constant, if the frequency is increased to 1 kHz, the contact angle further decreases (42°). Additional increases in the frequency to 10 kHz continue to suppress the contact angle to 14°. This justification is valid for every IL studied (see Table 2).

According to eq 2, at a fixed V and fixed f, ILs with different ϵ_{IL}, σ, γ, and d should generate different contact angles values (θ). Our experimental results agree with this as well. For example, the contact angles of the studied ILs at 1 kHz and 50 V are, 66° for [bmim][Cl], 57° for $[bmim][PF_6]$, 44° for $[bmim][NTf_2]$, 44° for $[bmpy][NTf_2]$, 47° for $[3C_6C_{14}P][DCA]$, 36° for $[3C_6C_{14}P][NTf_2]$, 43° for $[(bim)_2C_{10}][NTf_2]$, 48° for $[(beim)_3a][NTf_2]$, and 54° for $[(bimC_{10})_2im][NTf_2]$. Apart from the above-mentioned observations, there is another important phenomenon observed with the $\Delta\theta_S$ values. The $\Delta\theta_S$ values of

(35) Chatterjee, D.; Shepherd, H.; Garrell, R. L. *Lab Chip* **2009**, *9*, 1219–1229.

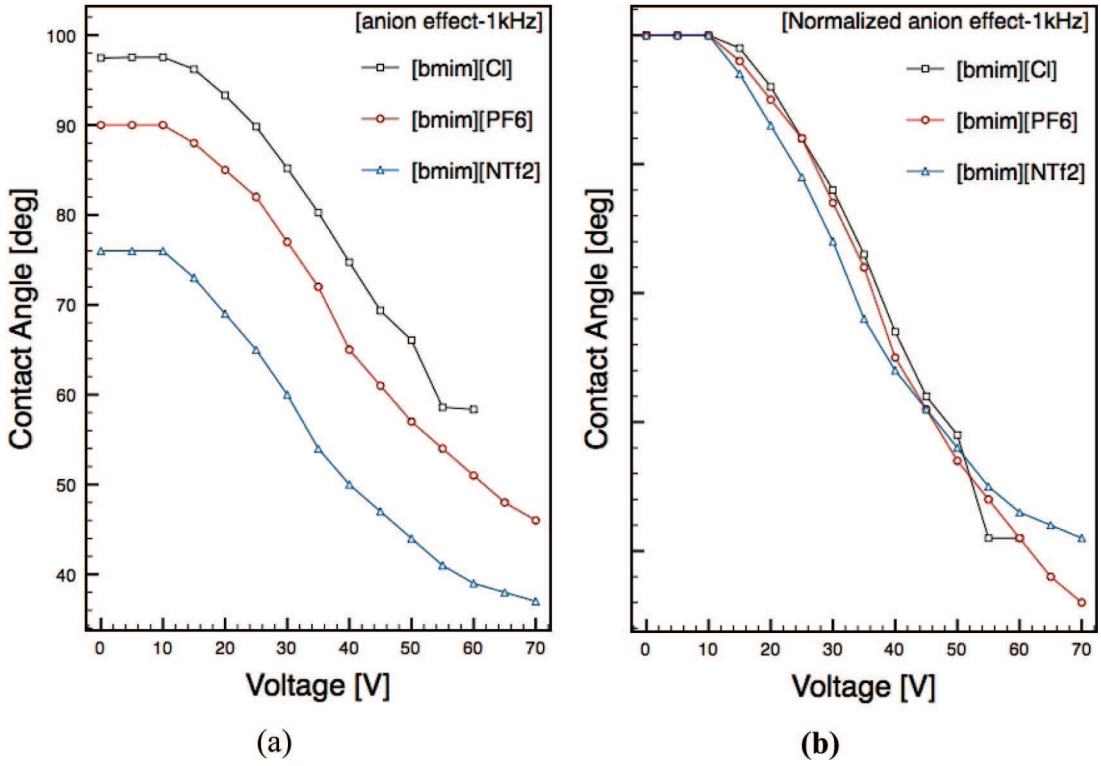

Figure 5. (a) Electrowetting curves of [bmim][Cl], [bmim][PF_6] and [bmim][NTf_2] at 1 kHz. (b) Electrowetting curves of [bmim][Cl], [bmim][PF_6], and [bmim][NTf_2] at 1 kHz were overlaid normal to the maximum θ_0 value.

[bmim][Cl], [bmpy][NTf_2], and [$(bimC_{10})_2$im][NTf_2] increase when the frequency increases from 60 Hz to 1 kHz, but it remained constant when the frequency increases from 1 to 10 kHz. (see Figure 4). Also for [$(beim)_3$a][NTf_2] those values at all three frequencies differ from one another by less than 4°. This phenomenon may be due to (1) the presence of critical frequency (f_C), (2) the effect of ordinary contact angle saturation, or (3) both.

Effect of the Critical Frequency (f_C). It is reported that at their f_C liquids tends to change from conductive to dielectric behavior.[35,36] When the frequency is lower than f_C, liquids behave as conductors, and when the frequency is higher than f_C liquids behave as insulators. For our system, f_C, can be written as[35]

$$f_C = F(R_{IL}, C_{IL}, C_T) \quad (3)$$

(See SI for the derivation) where, C is the capacitance and R is the resistance. The subscripts "IL" and "T" indicate the IL and Teflon layers, respectively. Since different ILs have different R_{IL} and C_{IL} values, according to eq 3, f_C values of each IL should differ from one another. When increasing the frequency, θ starts to decrease. However after $f = f_C$, the liquid becomes dielectric in nature and as a consequence the reduction in θ should stop or should exhibit very little change. Since the f_C for each IL will be different, the reduction of θ between different frequencies should vary.

Effect of Ordinary Contact Angle Saturation. Ordinary contact angle saturation is observed for both AC and DC electrowetting experiments. It has many origins as well as many proposed mechanisms and is not yet fully understood.[30] The primary focus on this study was not the understanding of the contact angle saturation or the effect of critical frequency. Therefore we can not quantify the contributions of these two possible effects on the above observed phenomenon.

Anion Effects. Figure 5a shows the electrowetting curves for [bmim][Cl], [bmim][PF_6], and [bmim][NTf_2] at 1 kHz. These three ILs are monocationic and have a common cation, $bmim^+$. The size of the anion and charge delocalization of the anion decreases in the order of $NTf_2^- > PF_6^- > Cl^-$ (diameters NTf_2^- ~7.57 Å, PF_6^- ~5.10 Å, Cl^- ~3.62 Å).[37] According to Figure 5a, θ_0 increases in the same order, giving the highest θ_0 for the IL with the smallest anion (Cl^-) and giving the lowest θ_0 for the IL with the largest anion (NTf_2^-). This is mainly due to differences in the surface tensions of the ILs (Table 1). It has been reported that, if the size and/or the charge delocalization of an anion (say X) is smaller than those of another anion (say Y), then the surface tension of IL with X anion is larger than that of the corresponding IL with the Y anion.[2] Therefore, Figure 5a represents the dependence of θ_0 on the size and charge delocalization of anion.

Figure 5b shows the electrowetting curves of [bmim][Cl], [bmim][PF_6] and [bmim][NTf_2] at 1 kHz which are overlaid normal to θ_0 value of [bmim][Cl]. According to Figure 5b the $\Delta\theta$ and $\Delta\theta_S$ values are approximately same for the three ILs. It has been reported that the anion has a significant effect on the $\Delta\theta_S$ value with positive DC voltages but not with negative DC voltages due to the anion and Teflon surface interactions in positive DC voltage experiments.[2] In AC voltage conditions

(36) Jones, T. B. *Langmuir* **2002**, *18*, 4437–4443.

(37) Berthod, A.; Kozak, J.; Anderson, J.; Ding, J.; Armstrong, D. *Theor. Chem. Acc.* **2007**, *117*, 127–135.

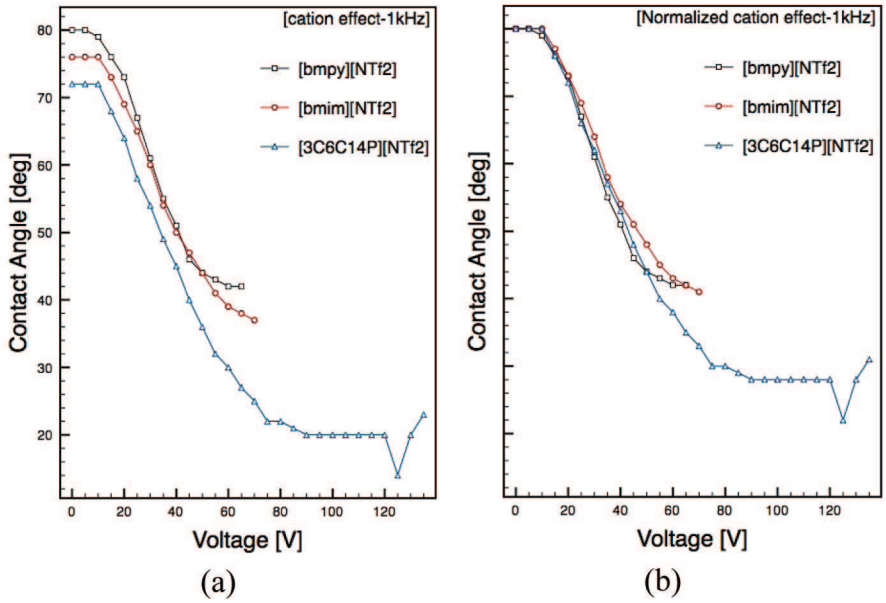

Figure 6. (a) Electrowetting curves of [bmpy][NTf_2], [bmim][NTf_2] and [$3C_6C_{14}P$][NTf_2] at 1 kHz. (b) Electrowetting curves of bmpy][NTf_2], [bmim][NTf_2], and [$3C_6C_{14}P$][NTf_2] at 1 kHz were overlaid normal to the maximum θ_0 value.

the Teflon surface and anion interactions are minimal.[26,29,31] Therefore, as expected for all frequencies with AC voltage, the $\Delta\theta$ and $\Delta\theta_S$ values are comparable for [bmim][Cl], [bmim][PF_6], and [bmim][NTf_2].

Cation Effects. Figure 6a shows the electrowetting curves of [bmpy][NTf_2], [bmim][NTf_2], and [$3C_6C_{14}P$][NTf_2] at 1 kHz. [bmpy][NTf_2], [bmim][NTf_2], and [$3C_6C_{14}P$][NTf_2] all have a common anion: [NTf_2]. Since [$3C_6C_{14}P$][NTf_2] has the largest cation, it has the lowest surface tension among the three ILs (Table 1). Even though, the [bmpy] cation and the [bmim] cation are approximately same size, the [bmpy] cation has a point charge whereas the [bmim] charge is delocalized over the imidazole ring. As a consequence [bmpy][NTf_2] has slightly larger surface tension value than that of [bmim][NTf_2]. These differences in surface tensions reflect on the θ_0 values (Figure 6a). This result is consistent with that of the anion effect which discussed in previous section.

Figure 6b shows the electrowetting curves for [bmpy][NTf_2], [bmim][NTf_2] and [$3C_6C_{14}P$][NTf_2] at 1 kHz, which are overlaid normal to their maximum θ_0 values. According to Figure 6b, all ILs have approximately the same $\Delta\theta$ values. Therefore it can be concluded that different cations have little effect on $\Delta\theta$ values. In contrast to the $\Delta\theta$, $\Delta\theta_S$ of [$3C_6C_{14}P$][NTf_2] is ~11° more than the $\Delta\theta_S$ of [bmpy][NTf_2] and [bmim][NTf_2] ILs. This observation can be explained by looking at stability of the ILs at higher voltages. ILs [bmpy][NTf_2] and [bmim][NTf_2] only stable up to 70 and 65 V at 1 kHz respectively, after which they tend to decompose or burn. However [$3C_6C_{14}P$][NTf_2] is stable at voltages even over 135 V (Table 3). Reasons for this decomposition or burning are discussed in the following section.

Stability of the ILs Under AC Voltages. The voltages at which ILs remain stable, are listed in Table 3. It is observed that, at higher frequencies, ILs become more vulnerable to decomposition. As an example, [$(beim)_3a$][NTf_2] remains stable up to 150 V when the frequency is 60 Hz, while at 1 kHz and 10 kHz it remains stable up to 140 and 70 V respectively (Table 3). A 10-fold increase in the frequency caused [$(beim)_3a$][NTf_2] to decompose at approximately half of the voltage (75 V versus 145 V). This probably is related to the "sonication effect" which is known to break cells and/or molecules using high frequency sound waves. In fact Oxley et al., have shown ILs do decompose when sonicated with 20 kHz frequency sound waves.[38] Apart from that, electrolysis of water which contained in ionic liquids or an electric breakdown could also cause decomposition of ILs at higher voltages.

Table 3. Stability of ILs in AC Voltage[a]

ionic liquid	maximum voltage at which liquid remain stable/V		
	60 kHz	1 kHz	10 kHz
[bmim][Cl]	60	55	40
[bmim][PF_6]	70	70	38
[bmim][NTf_2]	70	70	45
[bmpy][NTf_2]	65	65	35
[$3C_6C_{14}P$][DCA][b]	190	155	75
[$3C_6C_{14}P$][NTf_2][b]	140	135	85
[$(bim)_2C_{10}$][NTf_2]	110	100	50
[$(beim)_3a$][NTf_2]	150	140	70
[$(bimC_{10})_2im$][NTf_2]	125	120	75
water[c]	25	100	230

[a] These values are for ~260 nm thick Teflon layer electrowetting experiment. [b] Did not decompose, but sparking was observed for these ILs. [c] Did not decompose, but oscillations were observed.

In comparison to ILs, it is observed that water oscillates more readily at low frequencies than at higher frequencies (Table 3). This may be due to the low viscosity of water and its resonance frequency.[39]

Evaporation. It was observed that the water drop completely evaporated when it is exposed to the atmosphere for 45 min,

(38) Oxley, J. D.; Prozorov, T.; Suslick, K. S. *J. Am. Chem. Soc.* **2003**, *125*, 11138–11139.
(39) Oh, J. M.; Ko, S. H.; Kang, K. H. *Langmuir* **2008**, *24*, 8379–8386.

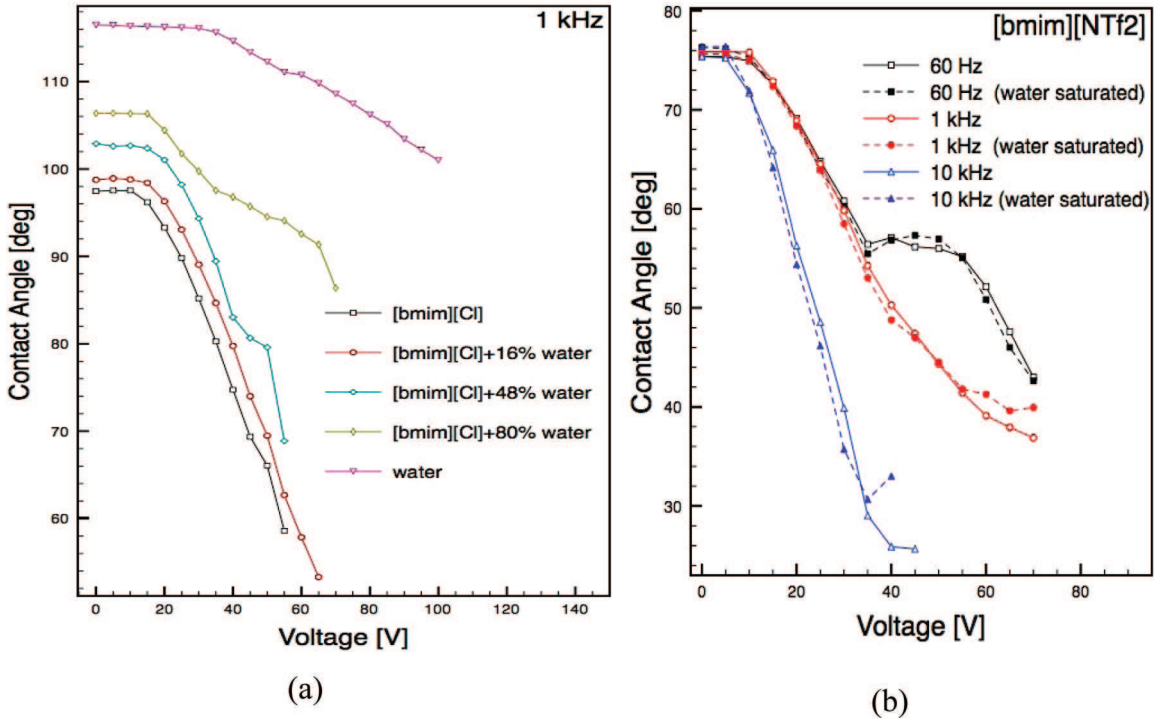

Figure 7. (a) Electrowetting curves of [bmim][Cl] and its diluted solutions at 1 kHz fequency. (b)Electrowetting curves of [bmim][NTf_2] and water saturated [bmim][NTf_2] at 60 Hz, 1 kHz and 10 kHz frequencies.

whereas, the volume of water-immiscible IL, [bmim][NTf_2], was unchanged after 45 min. The volume of water-miscible IL, [bmim][Cl], was slightly increased due to absorption of water from the atmosphere (see SI Figure S2.a). Similarly, the contact angle of the water drop changed rapidly with time, however the contact angle of all ILs remained constant for the entire experimental time (see SI Figure S2.b) This clearly shows the importance of using IL as the medium of EWOD based devices, which can be fabricated without any sealing and for long time period operations.

Effect of Water. Generally all liquids contain water to a certain extent. ILs are no exception. In the final step of IL synthesis, water and the other solvents were removed using a rotary evaporator as explained in the Experimental Section. To further minimize their water content, ~0.5 mL of each IL was stored in a vacuum oven for 12−18 h with phosphorus pentoxide (P_2O_5) at room temperature. Figure 7a shows the electrowetting curves of [bmim][Cl], DI water and 16%, 48% and 80% (w/w) water containing [bmim][Cl] solutions at 1 kHz frequency. According to Figure 7a an increase in the water content of [bmim][Cl] will result in an upward shift in the electrowetting curves toward that of pure water. Increasing the water percentage will increase the surface tension of a water miscible IL[2,40] and that will cause the electrowetting curves to shift upward. Electrowetting curves of [bmim][NTf_2] and its water saturated solution tested at 60 Hz, 1 kHz and 10 kHz frequencies, are shown in Figure 7b. For each frequency, approximately same curves can be observed for both [bmim][NTf_2] and its water saturated analogue. Therefore it can be concluded that a water has negligible effect on the AC electrowetting of water immiscible ILs. These results agree well with previous results published on effect of water on the DC electrowetting of ILs.[2]

Reversibility. The reversibility of two ILs ([bmim][Cl] and [bmim][NTf_2]) were tested at 1 kHz. Figure 8 (a) and (b) represent the electrowetting curves of [bmim][Cl] and [bmim][NTf_2] in three different experiments. The open symbols represent the contact angles of the ILs, five seconds after the voltage is switched off. The electrowetting process of these two ILs seems to be reversible to a great extent, that is, the drop returns close to its original contact angle value, the difference between original contact angle and the return contact angle values are approximately ~3−4°. Recent work by Restolho et al. demonstrated irreversibility of ILs in electrowetting at DC voltages.[21] Differences between our systems and theirs may be due to two reasons, (1) Surface roughness: reversibility is greatly affected by the surface roughness, with smoother surfaces having greater reversibility. However, there's no indication about their surface coating technique or surface treatments, therefore its difficult to compare the two systems. (2) Reversibility also can be affected by ion adsorption to the surface. It has been reported that in AC electrowetting ion adsorption to the surface is less than that in DC conditions.[26,31] Hence, better reversibility under AC voltage is logical. However, Restolho et al. suggested that "the irreversibility (or reversibility) of the electrowetting process is a consequence of the experimental procedure and does not reflect an intrinsic characteristic of the ionic liquid".[21] Here we confirm that statement and we believe that surface enhancement is more important in order to get higher reversibility than the changing the IL properties.

Edge Instability/Satellite Droplets. It has been reported that for aqueous electrolytes, edge instability is common under AC conditions, that is, small satellite droplets form next to the parent

(40) Liu, W.; Zhao, T.; Zhang, Y.; Wang, H.; Yu, M. *J. Solution Chem.* **2006**, *35*, 1337–1346.

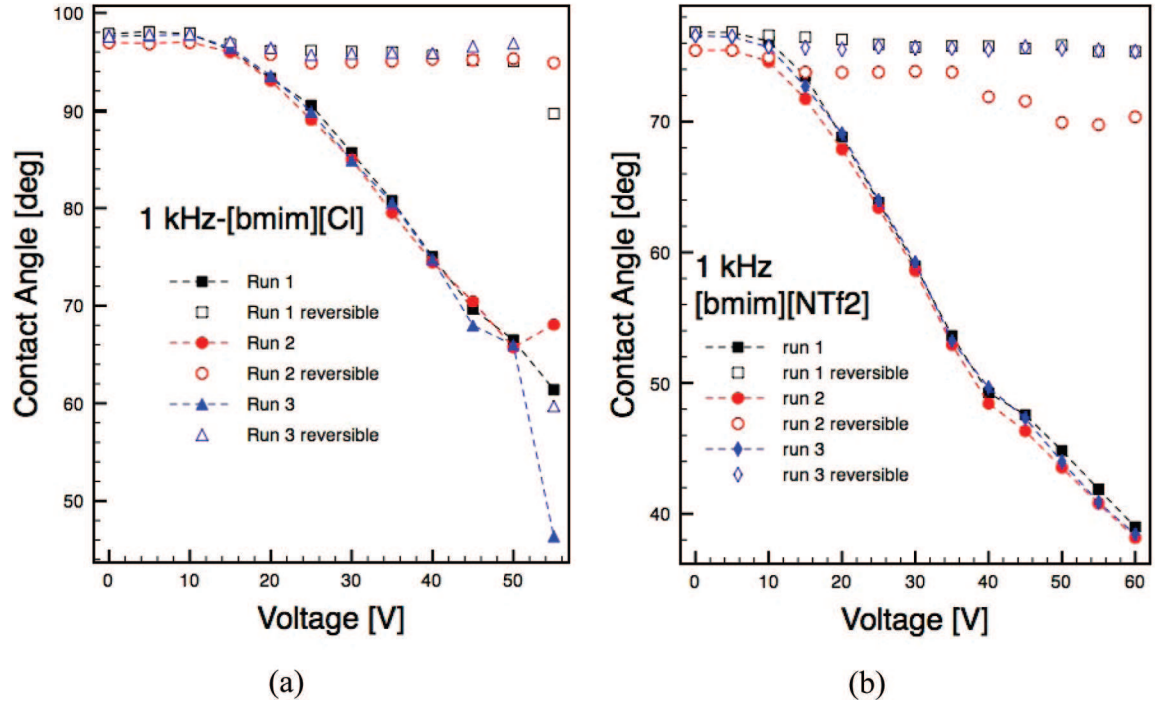

Figure 8. (a) Reversibility of [bmim][Cl] at 1 kHz (b) Reversibility of [bmim][NTf_2] at 1 kHz. Solid symbols represent contact angle at designated voltage and frequency. Open symbols represent the contact angles of the ILs, five seconds after the voltage is switched off.

droplet.[26,30,41] However with ILs satellite droplets were not observed. This is another advantage of ILs over aqueous electrolytes.

In addition to the above-mentioned observations, it was found that, when the electrowetting curves are overlaid at their maximum θ_0 values, at low frequency (60 Hz) normalized curves tends to coincide until their saturation points. Conversely at high frequency (10 kHz) the normalized curves seem to deviate from one another. (See SI Figure S12).

CONCLUSIONS

The apparent contact angle change ($\Delta\theta$) obtained by electrowetting was higher under AC voltage conditions than with DC voltage conditions for all ILs tested. The frequency of the AC voltage was directly related to $\Delta\theta$. Some ILs had 4−5 times larger $\Delta\theta$ with AC voltage conditions than with DC voltage conditions. At higher voltages, ILs seems to be more stable at lower frequencies than higher frequencies. ILs did not evaporate regardless of the length of the study, but all water drops completely evaporated in 45 min or less. Edge instability/ satellite-droplets were not observed for ILs in either AC or DC experiments. Reported physical properties and the AC electrowetting data of ILs can be used to optimize their use in EWOD based applications.

(41) Vallet, M.; Vallade, M.; Berge, B. *Eur. Phys. J. B* **1999**, *11*, 583–591.
(42) Breitbach, Z.; Armstrong, D. *Anal. Bioanal. Chem.* **2008**, *390*, 1605–1617.
(43) Page, P. M.; McCarty, T. A.; Baker, G. A.; Baker, S. N.; Bright, F. V. *Langmuir* **2007**, *23*, 843–849.
(44) McFarlane, D. R.; Sun, J.; Golding, J.; Meakin, P.; Forsyth, M. *Electrochim. Acta* **2000**, *45*, 1271–1278.
(45) Widegren, J. A.; Saurer, E. M.; Marsh, K. N.; Magee, J. W. *J. Chem. Thermodyn.* **2005**, *37*, 569–575.
(46) ILCO Ionic Lube. www.ilco-chemie.de/downloads/Ionic%20Liquid.pdf (accessed 09/27, 2009).

ACKNOWLEDGMENT

We thank Prof. Zoltan A. Schelly for providing the Karl Fischer Titrator and the Robert A. Welch foundation (Y0026) for financial support.

SUPPORTING INFORMATION AVAILABLE

Additional information as noted in text. This material is available free of charge via the Internet at http://pubs.acs.org.

Received for review June 22, 2009. Accepted February 22, 2010.

AC9021852